# Self-polymerization of carbonyl pigment for high-performance aqueous ammonium-ion battery

Jinyao Yang,[a] Wendi Wang,[b] Zeyu Cao,[a] Jingyuan Zhang,[a] Hang Ren,[a] Ying Yang,[a] huaiyu Shao,[c] and Shengyang Dong*[a,c]

[a] Jiangsu Key Laboratory of New Energy Devices & Interface Science, School of Chemistry and Materials Science, Nanjing University of Information Science and Technology, Nanjing 210044, China

E-mail: dongsyst@nuist.edu.cn

[b] ZIBO XINCAIIC CO., LTD, Zibo 255000, China.

[c] Institute of Applied Physics and Materials Engineering, University of Macau, Macau 999078, China

## Experimental section

Preparation of P420.

The organic anode material was prepared by annealing PTCDA at 420 °C for 3 h under Ar with a heating rate of 3 °C $min^{-1}$. The heat treated sample is marked as P420.

Preparation of Cu-HCF.

According to previous literature,[S1] $Cu_3[Fe(CN)_6]_2$ (Cu-HCF) was prepared via a simple co-precipitation method with $K_3[Fe(CN)_6]$ and anhydrous $CuSO_4$ as start precursors. Firstly, 1.6471 g $K_3[Fe(CN)_6]$ was dissolved in 50 mL deionized (DI) water to form solution A. Then, 1.5969 g anhydrous $CuSO_4$ was added in 50 mL DI water to form solution B. Lastly, under magnetometric stirring, solution A and solution B were added dropwise simultaneously to 100 mL DI water. The green precipitates were collected by centrifugation, washed with deionized water and ethanol, and then dried in a vacuum oven at 60 °C.

## Materials characterization

X-ray diffraction (XRD) was performed on a Rigaku Ultra 250 detector with Cu Kα radiation. The diffraction peaks were recorded from 5 to 70° with an interval of 0.02° and a sweep rate of 10° $min^{-1}$. The morphologies and microstructures were collected by scanning electron microscopy (SEM, ZEISS, Gemini300S). X-ray photoelectron spectroscopy (XPS, PerkinElmer PHI 550 spectrometer) was performed on an Al Kαsource. Fourier transform infrared (FT-IR) spectroscopy was carried out on a Shimadzu IR Prestige-21. Thermogravimetric analysis (TGA) was done on a TA STD650 thermal analyzer at a temperature ramp of 5 °C $min^{-1}$.

## Electrochemical measurements

All half-cell electrochemical tests were tested in three-electrode cells. The electrode material was composed of 70 wt% active material, 20 wt% carbon black and 10 wt % polyvinylidene fluoride binder (PVDF). Then, the slurry was coated on a 10 mm diameter carbon paper and dried overnight at 80 °C under vacuum. The active mass loading of the working electrode was 0.9~1.4 mg $cm^{-2}$. The counter electrode used was activated carbon (AC) films, in which AC, carbon black, and polytetrafluoroethylene (PTFE) were blended with a mass ratio of 8:1:1. The Ag/AgCl electrode (1 M KCl) was

used the reference electrode. As for ex situ XRD, FT-IR tests, we prepared P420 free-standing films as the working electrodes, which employed PTFE as the binder. The electrochemical window of Cu-HCF//P420 full battery is predicted to be 0.1~1.9 V (the mass ratio of Cu-HCF and P420 = 2:1). Before assembling the full battery, it is necessary to activate the Cu-HCF and P420 electrodes by cycling five times at 0.1 A $g^{-1}$, and then the Cu-HCF positive electrode (at discharged state) and the P420 negative electrode (at charged state) is assembled for the full battery test. All of the electrochemical tests were performed at room temperature.

Cyclic voltammetry (CV) was tested on the Corr Test CS-350 electrochemical work station. The galvanostatic charge−discharge (GCD) processes were performed on the LANBTS cell test system. The GITT was employed to figure out the diffusion coefficient of $NH_4^+$ by using a set of galvanostatic discharge pulses of 10 min at 0.1 A $g^{-1}$, followed by relaxing for 1 h. The $NH_4^+$ diffusivity reflects the kinetic behaviors of the cathode, and it was calculated with the following equation

$$D = \frac{4}{\pi\tau}\left(\frac{mv}{MS}\right)^2\left(\frac{\Delta E_s}{\Delta E_t}\right)^2 \quad (1)$$

where D ($cm^2$ $s^{-1}$) is the diffusion coefficient of $NH_4^+$. τ (s) corresponds to the constant current pulse time; m (g), M (g $mol^{-1}$), *v* ($cm^3$ $mol^{-1}$), and S ($cm^2$) represent the quality, molar mass, molar volume, and contact area of the electrode with the electrolyte of the active material, respectively; $\Delta E_S$ (V) is the change of steady-state voltage during the current pulse, and $\Delta E_t$ (V) represents the potential difference at a constant current subtracting IR drop.

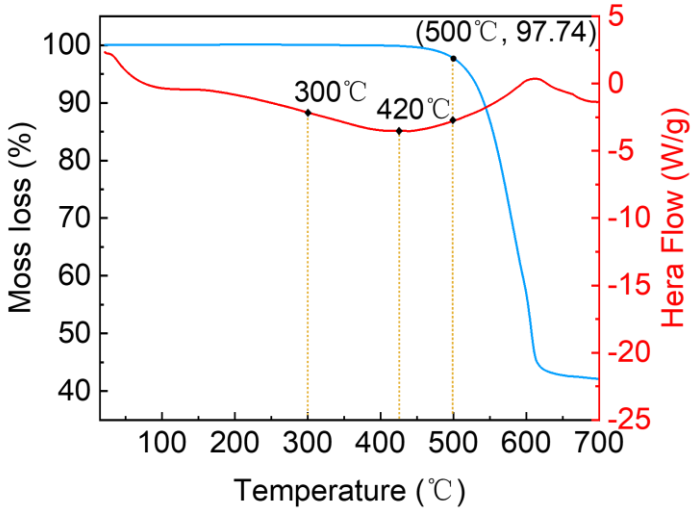


**Fig. S1** TGA/DSC curves of pristine PTCDA (300 ℃, 420 ℃ and 500 ℃ positions on the DSC curve).

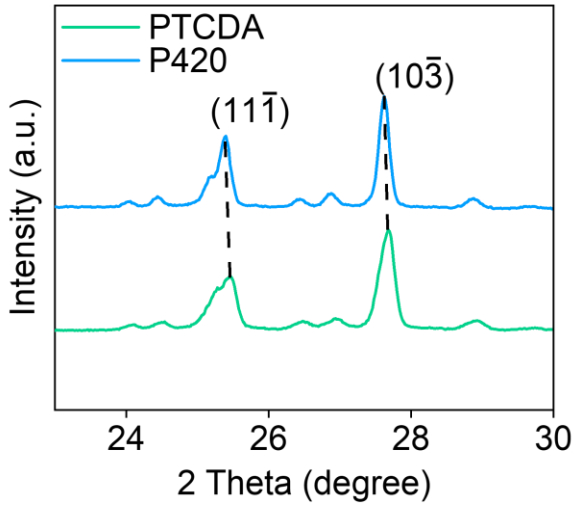


**Fig. S2** XRD patterns of pristine PTCDA and P420.

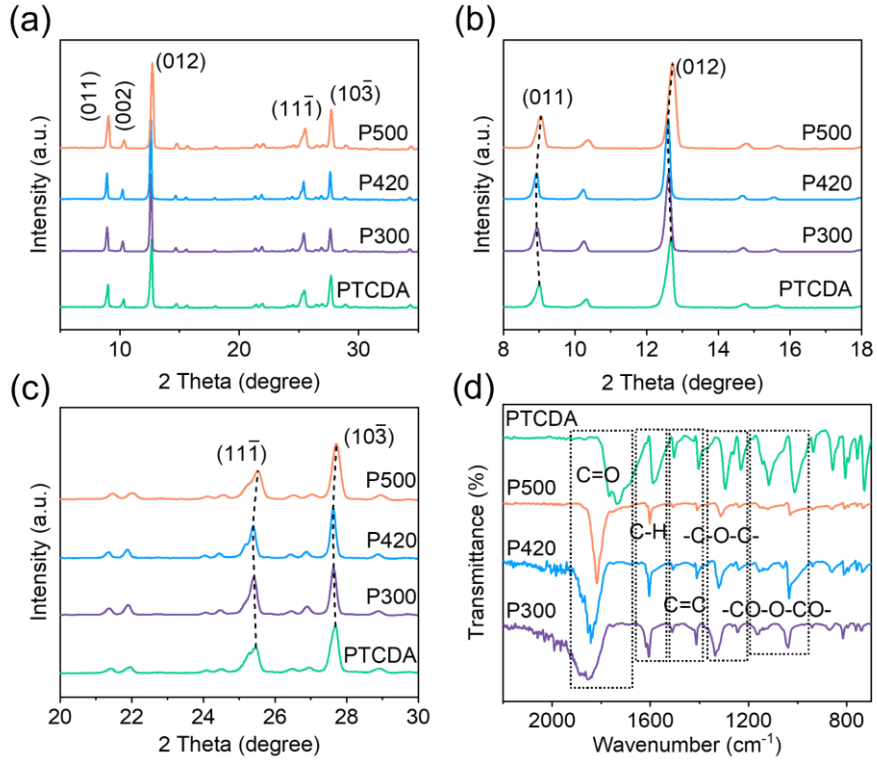


**Fig. S3** (a-c) XRD patterns and (d) FTIR spectra of pristine PTCDA, P300, P420 and P500.

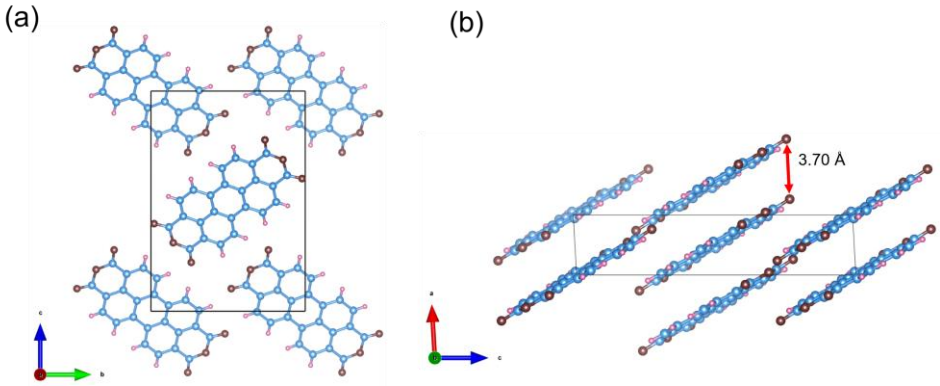


**Fig. S4** Crystalline structure of α-PTCDA. The blue, pink, and brown spheres represent C, H, and O atoms, respectively.

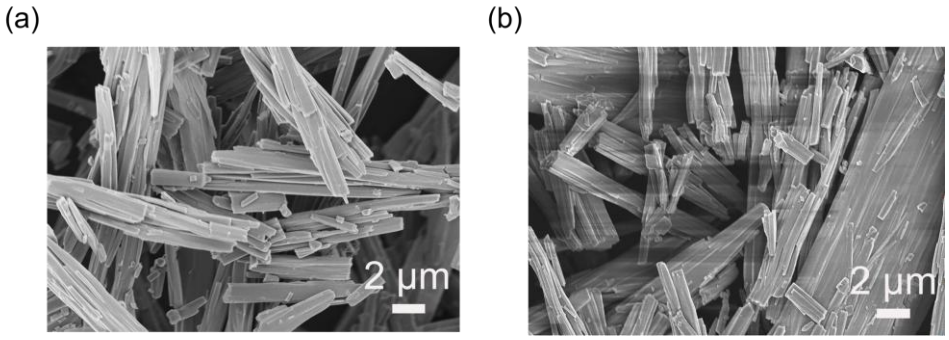


**Fig. S5** SEM images of (a) P300 and (b) P500.

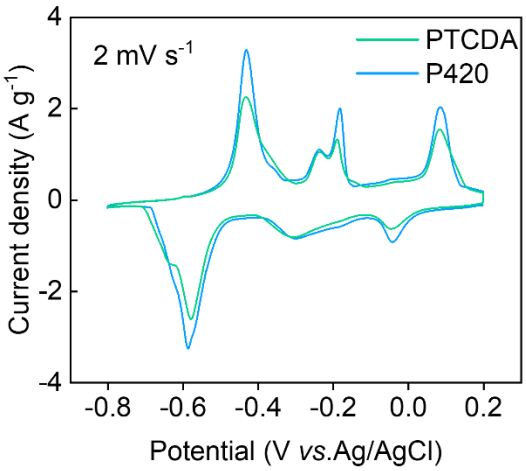


**Fig. S6** CV curves of PTCDA and P420 anodes at 2 mV $s^{-1}$.

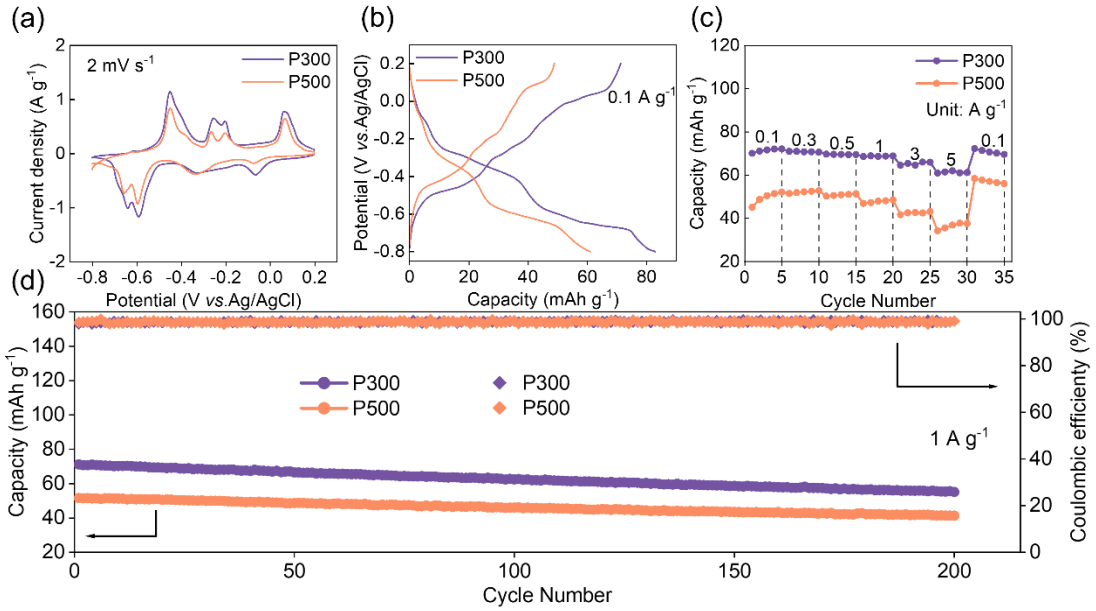


**Fig. S7** Electrochemical performance of P300 and P500 (a) CV profiles, (b) discharge/charge curves, (c) rate capability, and (d) cycling stability and coulombic efficiency.

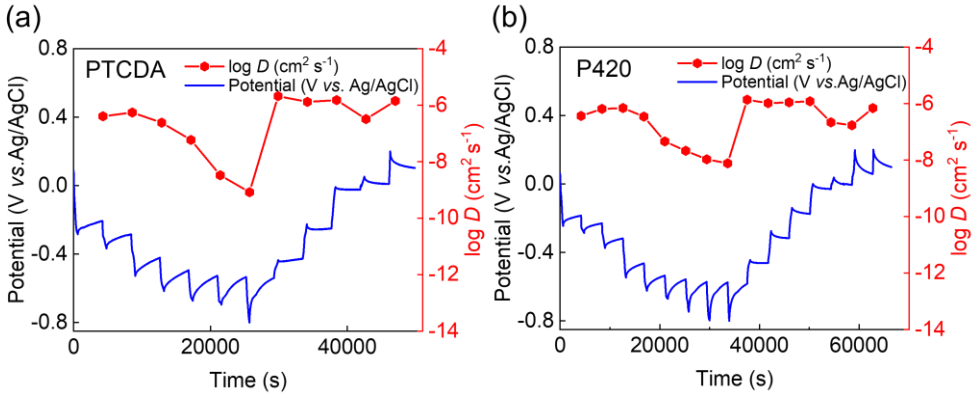


**Fig. S8** GITT test with corresponding diffusion coefficient of (a) pristine PTCDA and (b) P420.

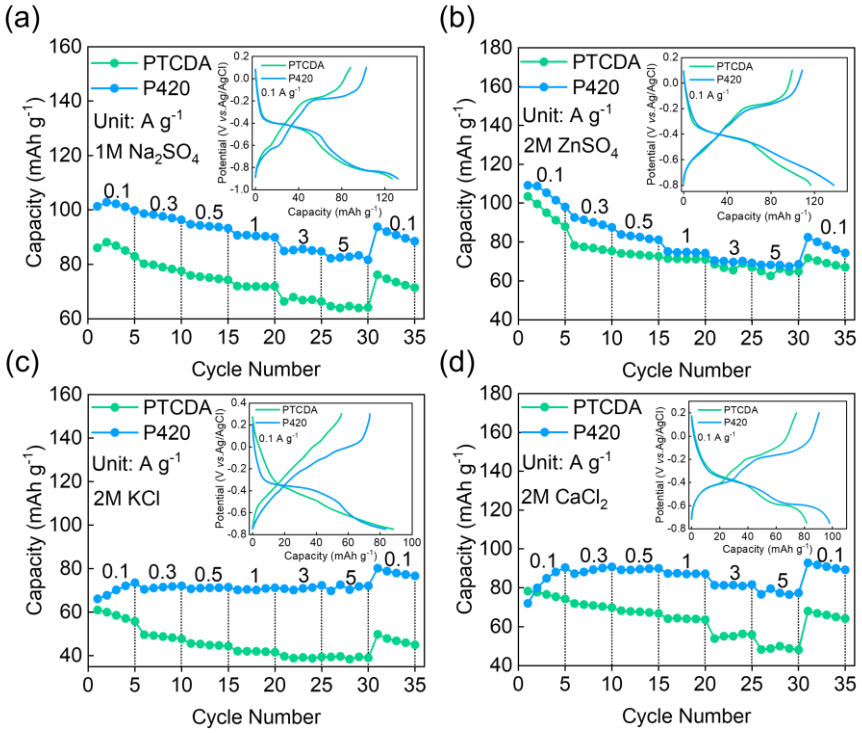


**Fig. S9** Rate capacities and GCD curves of different metal-ion electrolytes at pristine PTCDA and P420. (a) 1M $Na_2SO_4$. (b) 2M $ZnSO_4$. (c) 2M KCl. (d) 2M $CaCl_2$.

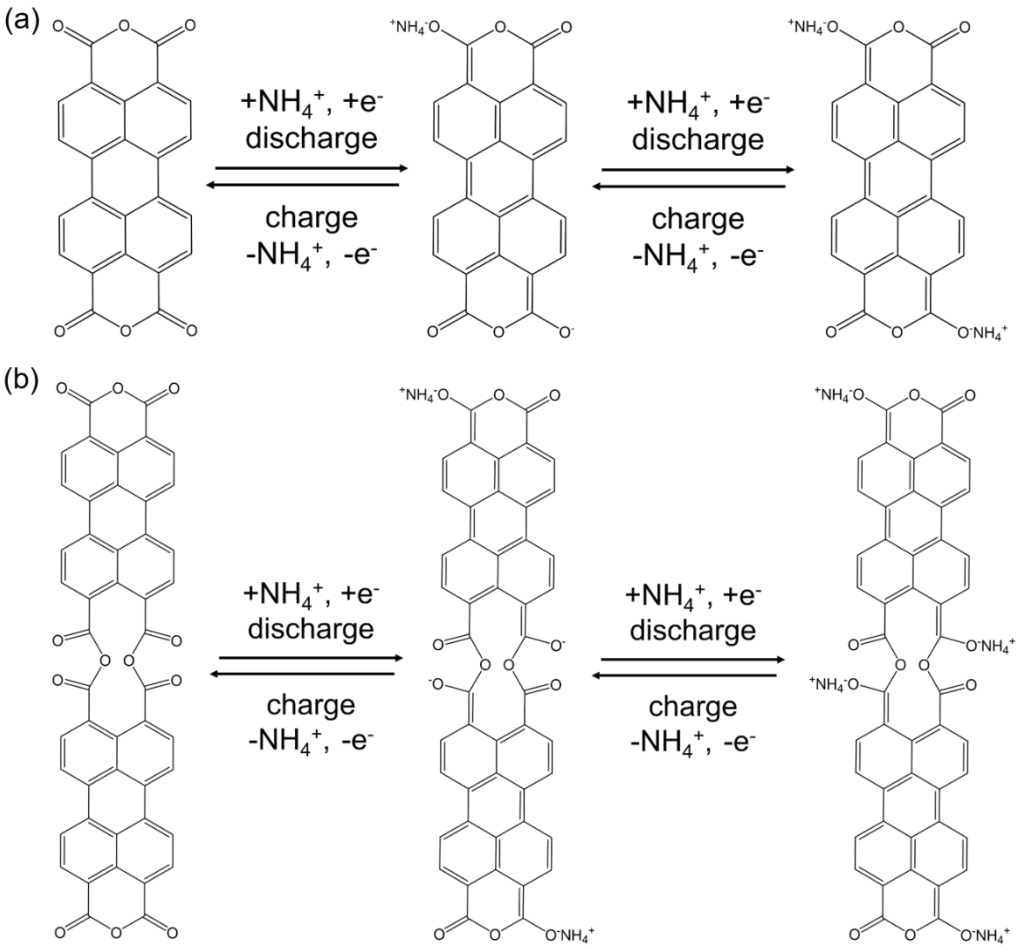


**Fig. S10** Proposed $NH_4^+$ incorporation mechanism of (a) PTCDA and (b) P420.

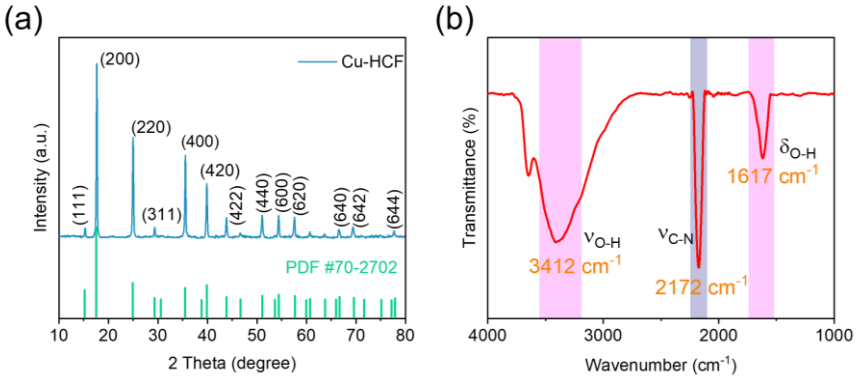


**Fig. S11** (a) XRD pattern and (b) FTIR spectrum of Cu-HCF.

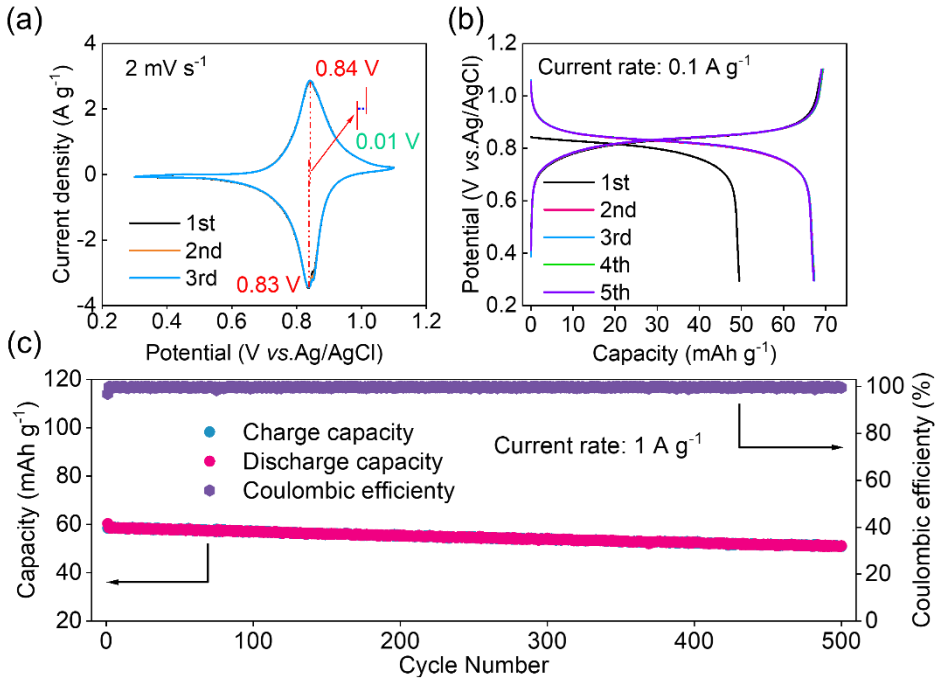


**Fig. S12** Electrochemical performance of Cu-HCF. (a) CV profiles, (b) discharge/charge curves, and (d) cycling stability and coulombic efficiency.

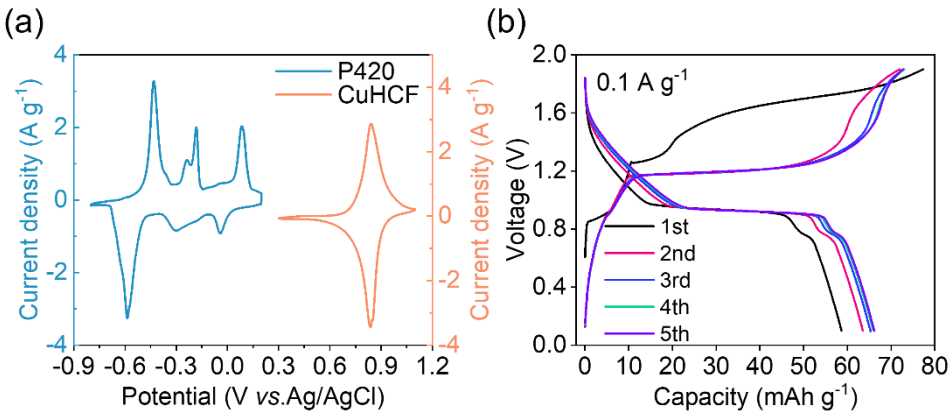


**Fig. S13** (a) CV curves of Cu-HCF cathode and P420 anode at 2 mV $s^{-1}$. (b) GCD profiles of the first five cycles at 0.1 A $g^{-1}$.

**Reference**

S1. X. Zhang, M. Xia, H. Yu, J. Zhang, Z. Yang, L. Zhang and J. Shu, *Nano-Micro Lett*, 2021, **13**, 139.